An Analysis of Viking S-X Doppler Measurements of Solar Wind Columnar Content Fluctuations

P. S. Callahan
Tracking Systems and Applications Section

More than 320 passes of Viking S-X Doppler data have been used to investigate columnar content fluctuations in the solar wind from 19 August, 1976 to 28 February, 1977. These data are used to estimate the power spectrum and radial dependence of solar wind density fluctuations. It is found that: (1) the electron density fluctuations decline with heliocentric distance as $r^{-1.8 \pm 0.1}$*; (2) the power spectrum depends on fluctuation frequency as* $\nu^{-2.5 \pm 0.2}$*. These results are used to predict range change as a function of time scale and sun-earth-probe angle. Changes of interest for advanced navigation techniques are found to be likely.*

I. Introduction

There is continuing interest in the errors introduced into radio metric tracking by the solar wind (SW) plasma. In order to estimate these errors a large amount of Viking S-X Doppler data measuring the change in electron columnar content has been analyzed. Because the density fluctuations (DF) are of a random nature the analysis has been done in terms of the power spectrum and the changes in spectral amplitude with heliocentric distance extracted.

A long term goal for the DSN is a predictive model of radio metric data quality. This analysis is a major first step in building that model as it provides the large-scale radial and time variations of the SW plasma. It remains to compare the residuals from these large-scale models to solar surface and other SW data to develop the detailed predictive model.

A preliminary report of the present analysis (but with only half the amount of data) was given in Ref. 1. The major differences between the findings there are (1) a revision of the spectral index from -3.0 to -2.5; and (2) a deletion of the discussion of sunspot cycle effects. It has become clear that a longer time base of measurements will be needed to discuss sunspot cycle effects.

The data coverage for this analysis is described in Section II. The analysis procedures are outlined in Section III. Section IV gives the results and discusses the implications for radio metric data.

II. Data Coverage

The data coverage for this analysis is shown in Table 1. The data are given in the groups in which they were averaged to determine the radial dependence of the power spectrum. The dates are in the format YYMMDDHH (year, month, day, hour at beginning of pass). Superior conjunction was taken to be 1976 November 25, 00 hours.

All of the passes used in this analysis were at least 5 hours long and contained at least 275 points. Thus, some gaps were allowed, but none exceeding 1 hour. Most of the data were 1-minute samples, but stretches of 10-second data occur in some passes. The net average sample spacings ranged from about 55 to 65 seconds. Individual passes lasted up to 12 hours. Near and after conjunction 10-second and some 1 second data were obtained in large amounts. Ten second data from 8 to 15 December 1976 have been included in this analysis by averaging the data to 30-second sample times and then treating the data to give the same spectral resolution as the 60 second passes. The 10 and 1 second data have been examined and show that the power spectrum continues smoothly to higher frequencies.

The coverage of one or both spacecraft is often continuous. When the doppler data overlap, it is possible to continue the record by continuing to add the change in columnar content at each step. Records up to 32 hours (typically 15-20 hours) have been constructed in this way. The spectra from these longer records have been averaged in the same way as the results presented here. These data show that the power spectrum also continues smoothly to lower frequencies.

Altogether more than 320 passes of S-X Doppler data ($\gtrsim$3000 hrs) have been analyzed. These data span ±95 days around superior conjunction and cover the range of heliocentric distances of closest approach of 0.031 to 0.487 AU. Continuous data records up to 32 hr and sample rates as fast as 1 per sec allow highly reliable estimates of the power spectrum in the frequency range 1×10^{-4} to 2×10^{-1} Hz.

III. Data Analysis

In order to investigate the columnar content changes under a wide range of conditions, it is necessary to have an objective measure of these changes. The power spectra of the data provide such a measure. The spectra give the mean squared fluctuation per unit frequency interval in a range of frequencies. Thus, given the power density at some frequency, $P_{\Delta I}(\nu)$, the expected change in the columnar content on a time scale $t_1 = 1/\nu$ is

$$\Delta I(t_1) \cong (P_{\Delta I}(\nu)^*\nu)^{1/2} \qquad (1)$$

where for rapidly falling spectra at low frequencies we have approximated the frequency interval $\Delta\nu$ (spectral resolution) by ν.

The frequencies over which one can obtain reliable estimates of the spectrum from discretely sampled records of limited length are $1/4\ \Delta t \geqslant \nu \gtrsim 10/T$, where Δt is the sample rate, and T is the length of the record. For most of the data used here 3×10^{-4} Hz $\lesssim \nu \lesssim 4 \times 10^{-3}$ Hz, corresponding to times scales of 4 minutes $\lesssim t_1 \lesssim$ 1 hour. The longer records produced by tying passes together permit the investigation of time scales of up to 3 hours, while 10-second data extend the time scale down to 40 seconds ($\nu \sim 2 \times 10^{-2}$ Hz), and 1-sec data to 4 sec ($\nu \sim 2 \times 10^{-1}$ Hz).

For some purposes (near-simultaneous ranging or the error of making uplink calibrations using a downlink-only measurement) the change of the columnar content on various time scales is of most interest. In other cases (two-station tracking or single station tracking of two separated spacecraft) the change of the SW density on various cale sizes is more important. The latter can be obtained from the former if the SW velocity is known. A typical SW velocity is 350-450 km s^{-1}. Since our data have no direct measurement of the velocity, scale sizes inferred using 400 km s^{-1} could be in error by up to 50 percent since the range of velocities is ~300-700 km s^{-1}. The results here are in terms of frequency.

The results below were obtained through the following steps:

(1) The columnar content change records from each pass were autocorrelated to 60 lags (~1 hour). The 10 second data were summed to ~30-second intervals and autocorrelated to 80 lags (~40 minutes).

(2) The cosine transform of the autocorrelation, smoothed with the Hanning window, was used to give the power spectrum.

(3) The individual power spectra were averaged in groups of 5 to 12. The data were grouped by the distance of the ray path's closest approach to the sun, Q. The lowest value of all the averaged points was subtracted to remove the noise.

(4) The slopes of the averaged spectra were obtained by hand. A number of estimates were made for each spectrum to determine the possible range. It is typically ±0.2. Account was taken of the fact that the spectral estimation program overestimates the power at low frequencies by a factor of 2 to 4.

None of the data have been corrected for the change in ionospheric columnar content. This change is generally $\lesssim$1.5 meters over a pass and so is much less ($\lesssim$10 percent) than the observed changes, except for some passes in August and September. Neglect of this correction is not thought to signifi-

cantly affect any of the final results. Care was taken, especially for data taken very near the sun, to insure that slipped cycles were not added to the columnar content change. Apparent columnar content changes greater than 2m/min were never allowed and in most cases tighter limits were imposed.

In addition to the power spectrum analysis, the individual and long records were examined for rms variation about the mean, peak-to-peak change, maximum rate of change, and character (slope, single or multiple "humps," and time scale of significant change) of the change. The numerical indices are all closely related to the power spectrum. The character of the change allows some investigation of changes on longer time scales than can be done formally with the power spectrum.

IV. Results and Discussion

From the general character of the columnar content changes, especially those seen on the long (tied) passes, one can see that the power spectra extend to low enough frequencies to pick up most of the important changes. Occasionally, there are slopes or "humps" with time scales of 8-12 hours, but these occur only about once per month. At the fastest sample rates, the character of the columnar content is very similar, though of reduced amplitude. Thus, the data from the power spectra provide a fairly complete and realistic description of the columnar content changes for time scales from 2 seconds to several hours.

The spectral index range for each averaged spectrum is given in the last column of Table 1. The indices were estimated by hand on plots of the averaged spectra. The average and standard deviation of the upper and lower estimates are respectively $\beta_u = 2.63 \pm 0.18$, $\beta_L = 2.40 \pm 0.16$. The value $\beta = 2.5 \pm 0.2$ will be adopted for the spectral index of columnar content fluctuations. It is in good agreement with Ref. 2 and 3 and other recent work on SWDF. Examination of averaged spectra of data records in which passes were tied together to give total record lengths of 20-30 hr show that this spectral index is maintained down to $\nu \cong 1 \times 10^{-4}$ Hz. As discussed above the spectral estimation program overestimates the power at low frequencies. This effect is important, (approximately a factor of 2) at 3×10^{-4} Hz for single pass records. Thus, for reliable results the scaling law $\nu^{-2.5}$ should only be applied to $P(F2 = 6 \times 10^{-4}$ Hz) data in Table 1.

Data sampled at once per second and once per 10 sec were used to investigate the high frequency portion of the spectrum. It was found that at the highest frequencies, $1 \times 10^{-2} \lesssim \nu \lesssim 2 \times 10^{-1}$, the spectrum flattened somewhat to $2.1 \lesssim \beta \lesssim 2.3$. Below $\nu \cong 1 \times 10^{-2}$ Hz the spectral index remained at $\beta \cong 2.5$. Three sets of 1 sec. data (of 6 obtained) showed discrete spectral features at frequencies of about 1.5×10^{-1} Hz. The periodic (period $\cong 7$ sec) disturbances lasted for about 1 hour in each case. The spectral amplitude indicates columnar content changes of about 9×10^9 cm^{-2} = 8×10^{-4} m(!) of one-way S-band range change. The explanation of the features has not been found.

In Fig. 1, the averaged power density 3×10^{-4}Hz is plotted against Q, the distance of the ray path's closest approach to the sun. The line through the points has slope 2.6. Note that the Mariner points generally lie above the Viking points. The points at large Q may be biased upward by the ionosphere. These data overestimate the true spectral amplitude by a factor of 2.

To investigate the radial dependence more quantitatively, a computer program was used to find the RMS deviation about a series of models characterized by a radial exponent, γ and an ellipticity ϵ. The ellipticity was included because the solar corona is known to be reduced near the poles at sunspot cycle minimum. The model used was

$$P^{(\nu)}_{\text{scaled}} = P^{(\nu)}_{\text{obs}} \, (\text{Q}/0.1 \text{ AU})^{(3+2\gamma)} (1 + \epsilon \sin (\text{Lat}))^2 \tag{2}$$

where Q is the distance of closest approach (column 5 of Table 1) and Lat is the heliographic latitude of the point of closest approach (column 6 of Table 1). The parameters which produce the smallest RMS of the scaled spectral estimates about their average were $\gamma = -0.2 \pm 0.1$ and $\epsilon = 0.6 \pm 0.6$. The data show no strong preference for any value of ϵ, but do clearly show that γ is less than 0.

A decline of the spectral amplitudes of $Q^{-2.6}$ implies (for an approximately constant radial SW velocity) that SWDF decline as $\delta n \propto r^{-1.8 \pm 0.1}$. This result is also found in an analysis of Doppler Noise data (Ref. 3 and 4). It implies that the relative density changes become larger with radius, (since n declines at least as fast as r^{-2}), although this conclusion may be modified somewhat by including the acceleration of the SW near ($r \sim 3$ to $30 R_\odot = 0.015$ to 0.15 AU) the sun.

The data in Table 1 are well-summarized by the function

$$P(\nu,Q) = (4.0 \pm 2.0) \times 10^{30} \left(\frac{\text{Q}}{0.1\text{AU}}\right)^{-2.6 \pm 0.1} \left(\frac{\nu}{3 \times 10^{-4}}\right)^{-2.5 \pm 0.2} \text{cm}^{-4}\text{Hz}^{-1} \tag{3}$$

where Q is the distance of the ray path's closest approach to the sun, and ν is the frequency of the fluctuations in the columnar content, for $1 \times 10^{-4} \lesssim \nu \lesssim 1 \times 10^{-2}$ Hz, $0.03 \lesssim Q \lesssim 0.5$ AU. By using Eq. (1), one may easily deduce the rms change in columnar content from Eq. (3). The result in one-way meters of S-band range change is

$$\Delta I_{rms}(\tau,Q) = (0.039 \pm 0.019)\left(\frac{Q}{0.1\ \text{AU}}\right)^{-1.3}\left(\frac{\tau}{10\ \text{sec}}\right)^{0.75}\ \text{m} \tag{4}$$

where $\tau = 1/\nu$ is the time scale of changes.

Values of this expression for several values of τ and Q are given in Table 2. The distance scales ℓ in Table 2 are obtained by multiplying τ by a typical SW velocity of 400 km s^{-1}

The range changes in Table 2 could be significant for advanced navigation techniques. As the data of Table 1 and Fig. 1 show, the amplitude of the power spectrum is highly variable. Values 2 to 3 times those in Table 2 are possible on occasion (once per week to once per month). Furthermore, peak-to-peak changes between adjacent samples are $\cong 3\Delta I_{rms}$. Thus, overall changes between data points separated in time or from ray paths separated in space could be 3 to 10 times the values in Table 2. At SEP angles of 15° one might expect differences of 1.0 to 3.7 m on alternate range points separated by 15 min and of 0.03 to 0.1 m in VLBI data on a single source.

The differences expected in ΔVLBI will be $\sim \sqrt{2}$ greater than those for VLBI of a single source independent of the separation of the two sources in the sky because of the small error between the two ray paths to each source. The error introduced into alternate ranging could be significant, while the SW is virtually eliminated as an error source by ΔVLBI.

Reference

1. Callahan, P. S., "A Preliminary Analysis of Viking S-X Doppler Data and Comparison to Results of Mariner 6, 7, and 9 DRVID Measurements of the Solar Wind Turbulence," in the Deep Space Network Progress Report, 42-39, pp. 23-29; 1977, June 15.
2. Woo, R., "Radial Dependence of Solar Wind Properties Deduced from Helios 1/2 and Pioneer 10/11 Radio Scattering Observations," Astrophys, J., *219*, 727; 1978, January 15.
3. Callahan, P. S., "A First-Principles Derivation of Doppler Noise Expected from Solar Wind Density Fluctuations," in the Deep Space Network Progress Report 42-42, pp. 42-53; 1977, December 15.
4. Berman, A. L., "Viking S-Band Doppler RMS Phase Fluctuations Used to Calibrate the Mean 1976 Equatorial Corona," in the Deep Space Network Progress Report 42-38, p. 152.

Table 1. Averaged spectra of Viking S-X doppler data*

First Date	Last Date	No. Avg	SC	Q Avg (0.1AU)	Avg Lat	Obs P(F1) [a]	Obs P(F2) [b]	Days from Sup. Conjunction First	Last	Avg	P(F1), Scaled for Radial	Radial + Lat	P(F2), Scaled for Radial	Radial + Lat	β
76082116.	76082616.	10.	30.	4.870	3.0	.137+30	.124+29	-95.33	-90.33	-92.83	.4096+30	.3668+30	.3707+29	.3320+29	2.55-2.65
76082708.	76090100.	11.	30.	4.590	3.4	.788+29	.718+28	-89.67	-85.00	-87.33	.2044+30	.1846+30	.1862+29	.1682+29	2.7 -2.9
76090117.	76090616.	10.	30.	4.300	3.8	.164+30	.180+29	-84.29	-79.33	-81.81	.3637+30	.3315+30	.3992+29	.3638+29	2.5 -2.7
76090708.	76091016.	6.	30.	4.070	4.1	.142+30	.115+29	-78.67	-75.33	-77.00	.2760+30	.2533+30	.2235+29	.2052+29	2.5 -2.7
76090916.	76091522.	12.	27.	3.830	4.4	.690+29	.649+28	-76.33	-70.08	-73.21	.1159+30	.1071+30	.1090+29	.1008+29	2.3 -2.6
76091700.	76092121.	11.	27.	3.500	4.8	.446+30	.452+29	-69.00	-64.12	-66.56	.6035+30	.5627+30	.6116+29	.5703+29	2.3 -2.55
76101808.	76102721.	8.	30.	1.690	6.2	.229+31	.323+30	-37.67	-28.13	-32.90	.5399+30	.5194+30	.7615+29	.7326+29	2.5 -2.75
76102011.	76103111.	8.	27.	1.490	6.2	.136+31	.103+30	-35.54	-24.54	-30.04	.2370+30	.2278+30	.1795+29	.1726+29	2.3 -2.7
76110100.	76111320.	9.	30.	.960	5.4	.536+31	.506+30	-24.00	-11.17	-17.58	.3252+30	.3071+30	.3070+29	.2899+29	2.4 -2.6
76110121.	76110721.	7.	27.	1.070	5.9	.609+31	.638+30	-23.12	-17.12	-20.12	.4794+30	.4578+30	.5022+29	.4796+29	2.35-2.65
76112619.	76120220.	7.	20.	.280	-22.0	.113+33	.127+32	1.79	7.83	4.81	.3749+30	.5244+30	.4214+29	.5894+29	2.25-2.35
76120800.	76121522.	8.	20.	.908	-12.1	.187+32	.677+30	13.00	20.92	16.96	.9927+30	.1092+31	.3594+29	.3953+29	2.6 -2.8
76123119.	77010503.	6.	30.	1.910	-10.2	.153+31	.214+30	36.79	41.12	38.96	.4839+30	.5092+30	.6768+29	.7122+29	2.6 -2.85
77010416.	77010901.	5.	30.	2.040	-10.0	.226+31	.205+30	40.67	45.04	42.85	.8371+30	.8769+30	.7593+29	.7954+29	2.6 -3.0
77010518.	77010803.	5.	27.	2.060	-10.0	.570+30	.800+29	41.75	44.12	42.94	.2161+30	.2264+30	.3033+29	.3178+29	2.3 -2.4
77011100.	77011205.	5.	27.	2.280	-9.7	.457+30	.515+29	47.00	48.21	47.60	.2211+30	.2300+30	.2491+29	.2592+29	2.4 -2.7
77011218.	77011516.	5.	30.	2.360	-9.6	.121+30	.112+29	48.75	51.75	50.25	.6358+29	.6600+29	.5885+28	.6109+28	2.35-2.5
77011823.	77012014.	5.	30.	2.620	-9.2	.357+30	.311+29	54.96	56.58	55.77	.2411+30	.2479+30	.2100+29	.2160+29	2.3 -2.45
77013122.	77020818.	8.	27.	3.330	-8.0	.134+31	.282+29	67.92	75.75	71.83	.1609+31	.1610+31	.3386+29	.3388+29	2.35-2.6
77021518.	77022315.	8.	27.	3.870	-6.8	.630+30	.518+29	82.75	90.63	86.69	.1085+31	.1058+31	.8921+29	.8696+29	2.1 -2.3
77022200.	77022818.	7.	27.	4.070	-6.3	.135+30	.278+29	89.00	95.75	92.37	.2024+30	.2530+30	.5403+29	.5209+29	2.1 -2.4

a) F1 = 3 x 10^{-4} Hz

b) F2 = 6 x 10^{-4} Hz

*The scaled spectral estimates have been scaled by $(Q/0.1\ AU)^{2.6}$ and/or $(1 + 0.6 \sin(Lat))^2$ and then divided by the average of these factors (19.46 and 1.19) for the whole data set.

Table 2. ΔI_{rms} (τ, Q) in one-way S-band meters.
$\ell = \tau \times$ 400 km/sec

τ(sec) =		3000	1000	100	30	10	3
ℓ(km) =		1.2^{+6}	4^{+5}	4^{+4}	1.2^{+4}	4^{+3}	1.2^{+3}
Q(AU)	SEP	ΔI_{rms} (m)					
.05	2.9	6.86	3.01	.535	.217	.0952	.0386
.10	5.7	2.79	1.22	.217	.0881	.0386	.0157
.15	8.6	1.64	.721	.128	.0520	.0228	.0092
.20	11.5	1.13	.496	.0883	.0358	.0157	.0064
.25	14.5	.846	.371	.0660	.0268	.0117	.0048
.30	17.5	.668	.293	.0521	.0211	.0093	.0038
.40	23.6	.459	.201	.0358	.0145	.0064	.0026
.50	30.0	.344	.151	.0268	.0109	.0048	.0019

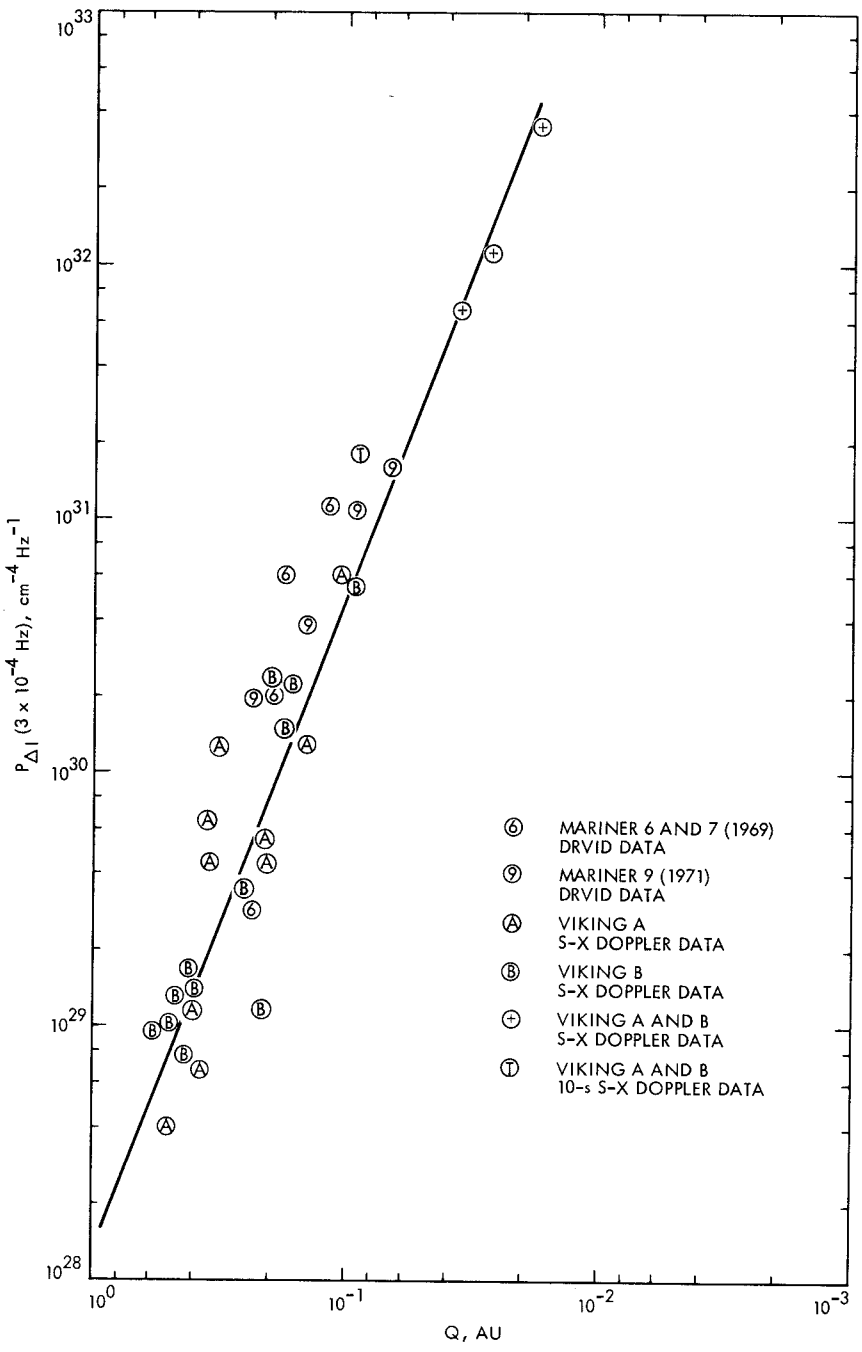

Fig. 1. Averaged spectral amplitudes